

RSC Advances



This is an *Accepted Manuscript*, which has been through the Royal Society of Chemistry peer review process and has been accepted for publication.

Accepted Manuscripts are published online shortly after acceptance, before technical editing, formatting and proof reading. Using this free service, authors can make their results available to the community, in citable form, before we publish the edited article. This *Accepted Manuscript* will be replaced by the edited, formatted and paginated article as soon as this is available.

You can find more information about *Accepted Manuscripts* in the [Information for Authors](#).

Please note that technical editing may introduce minor changes to the text and/or graphics, which may alter content. The journal's standard [Terms & Conditions](#) and the [Ethical guidelines](#) still apply. In no event shall the Royal Society of Chemistry be held responsible for any errors or omissions in this *Accepted Manuscript* or any consequences arising from the use of any information it contains.

Cite this: DOI: 10.1039/c0xx00000x

www.rsc.org/xxxxxx

ARTICLE TYPE

Biomimetic molecular organization of naphthalene diimide in the solid state: tunable (chiro-) optical, viscoelastic and nanoscale properties†

M. Pandeewar,^a Harshavardhan Khare,^b Suryanarayananarao Ramakumar,^b and T. Govindaraju^{*a}

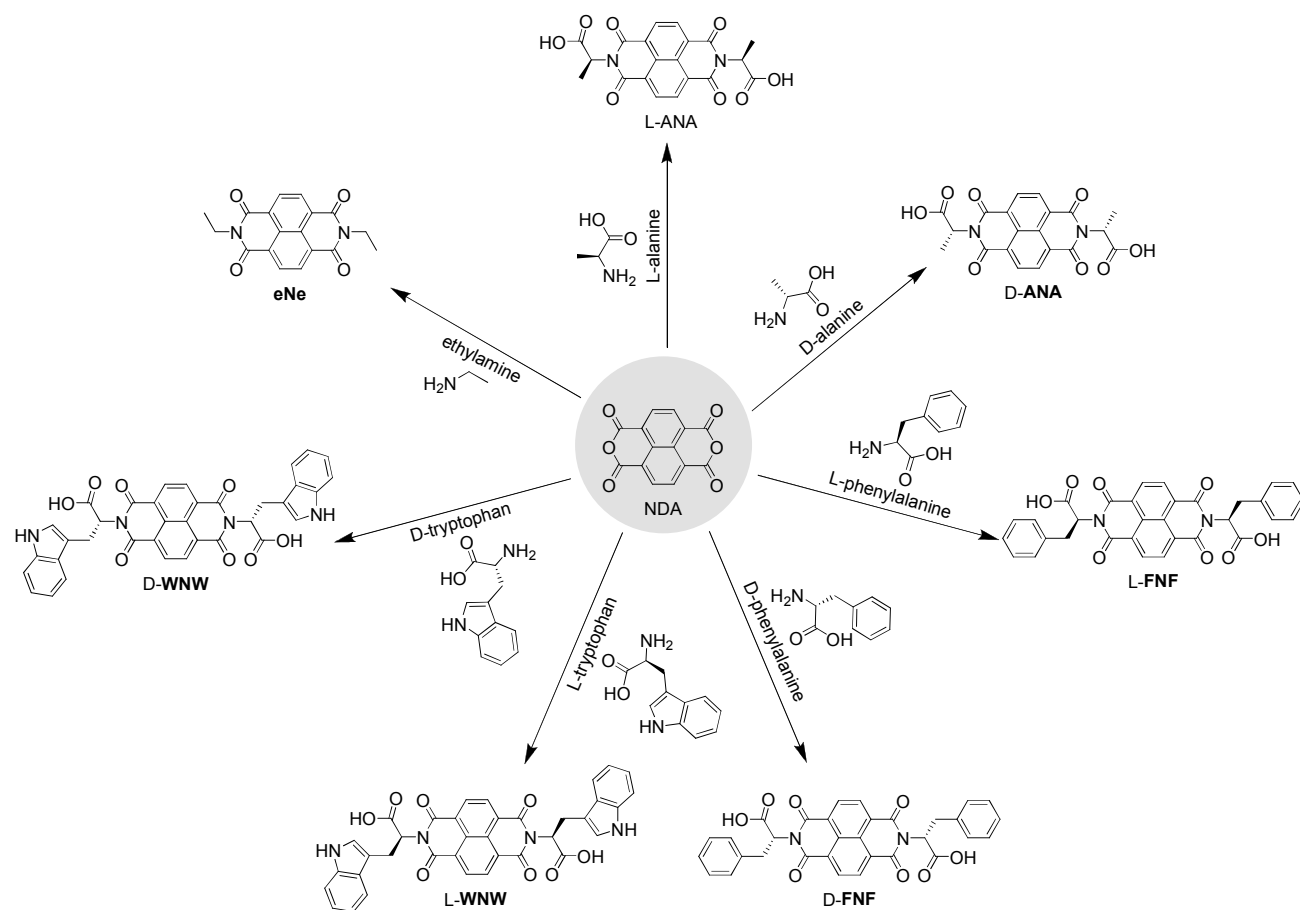
ABSTRACT: The interfacing of aromatic molecules with biomolecules to design functional molecular materials is a promising area of research. Intermolecular interactions determine the performance of these materials and therefore, precise control on the molecular organization is necessary to improve functional properties. Herein we describe the tunable biomimetic molecular engineering of promising n-type organic semiconductor, naphthalene diimide (NDI), in the solid state by introducing minute structural mutations in the form of amino acids with variable C α -functionality. For the first time we could achieve all the four possible crystal packing modes namely cofacial, brickwork, herringbone and slipped stacks of NDI system. Furthermore, amino acid conjugated NDIs exhibit ultrasonication induced organogels with tunable visco-elastic and temperature responsive emission properties. The amino acid-NDI conjugates self-assemble into 0D nanospheres and 1D nanofibers in their gel state while ethylamine-NDI conjugate forms 2D sheets from its solution. Photophysical studies indicated remarkable influence of molecular ordering on the absorption and fluorescence properties of NDIs. Interestingly, the circular dichroism (CD) and X-ray diffraction (XRD) studies revealed the existence of helical ordering of NDIs in both solution and solid state respectively. The chiral amino acids and their conformations with respect to the central NDI core are found to influence the nature of helical organization of NDIs. Consequently, the origin of preferential handedness in the helical organization is attributed to transcription of chiral information from amino acid to NDI core. On account of these unique properties, the materials derived from NDI-conjugates might find wide range of future interdisciplinary applications from materials to biomedicine.

Introduction

The nature and geometry of noncovalent aromatic interactions play an important role in chemistry, biology, and materials science.^{1,2} They are responsible for structure and function of DNA, several peptides and proteins, and are believed to be one of the main driving forces in aggregation of amyloid β to form toxic plaques of Alzheimer's disease.¹ Similarly, aromatic interactions are fundamental to design and development of optoelectronic systems in the area of organic electronics and biomaterials.² The experimental and theoretical investigations have provided clear evidence for the role of van der Waals, hydrophobic and electrostatic forces in the existence and stability of aromatic interactions.³ Nature-inspired chiral alignment of aromatic molecules has been attracting great interest owing to their fascinating structural features and relationship to biological structures. This concept has been effectively employed in various potential applications like understanding of Nature's mysterious selection of homochirality, designing of biomimetics, chiroptical switching, chiral sensing, separation and catalysis.⁴ During the past few years, considerable attention has been focused on the design and induction of helical bias in rigid aromatic molecules, polymers and small molecules by utilizing steric effects and noncovalent interactions.^{5,6} Interestingly, helical columnar stacks have emerged as promising molecular organizations for

optoelectronic applications by displaying exceptional charge carrier mobilities and exciton diffusion along the stacking columnar axis.⁷ Furthermore, the rational design of high performance organic electronic devices also need in-depth knowledge of structure and mode of molecular organization which remains to be understood. In this context, there has been a great interest in the low-molecular-weight (LMW) gels and single crystals. Their ordered and frozen molecular orientations lead to general understanding of fundamental chemical aspects behind the structural design to achieve desired molecular interactions and their impact on the properties.^{8,9} Consequently, substantial efforts have been devoted to the investigation of various types of packing modes of the p-type (HT: holes transport) organic semiconductor molecules for analyzing intermolecular charge transport property.⁹ However, the progress of n-type (ET: electrons transport) organic semiconductor molecules are still lagging behind p-type organic semiconductors.¹⁰ This necessitates the immediate need for studying n-type organic semiconductor molecular organization to improve their properties, in both academic and industrial research.

Rylene diimides are one of the extensively studied class of n-type organic semiconductor materials.¹⁰ Among them naphthalene diimide (NDI) has attracted special attention due to its molecular planarity, high π -acidity, well defined redox behavior, optical properties and wide range of applications from



Scheme 1 Molecular structures of NDI derivatives of chiral amino acids (L-ANA, L-FNF, L-WNW, D-ANA, D-FNF and D-WNW) and achiral ethylamine (eNe) synthesized by conjugating with 1,2,5,8-naphthalenetetracarboxylic dianhydride (NDA).

materials to biomedicine.¹¹ However, the key daunting challenges in controlling solid state molecular ordering with helical intermolecular organization remain to be addressed to further the advancement in NDI based materials for technological applications. Very recently, bio-inspired approaches has been reported, employing biological elements as chiral assembly directing substituents to design supramolecular systems and nanomaterials with diverse structural, chemical and chiroptical properties.^{41,12-15} This novel design based on the marriage between biomolecules and π -conjugated organic systems (e.g., NDIs) not only envision the engineering of helical molecular ordering through various noncovalent interactions but also synergistically combines the properties of constituent components.¹⁶ With this objective, we have chosen amino acids as self-assembly directing groups due to their inherent ability to make complex molecular architectures in biological systems and variable α -functionality can endow hydrophilic, hydrophobic and aromatic interactions in a single compact moiety. We methodically designed NDI bolaamphiphiles using enantiomeric amino acids with α -functionalities as aliphatic (alanine, ANA), aromatic (phenylalanine, FNF), heterocyclic/heteroaromatic (tryptophan, WNW) and NDI with flexible achiral ethylamine (eNe) (Scheme 1). Herein, we show the biomimetic molecular engineering of NDIs ordering in the solid state by introducing

25 minute structural mutations in the form of amino acids with variable α -functionality. For the first time we demonstrate all the four possible crystal packing modes *viz.* cofacial, brickwork, herringbone and slipped stacks (Fig. 1) with helical ordering of NDI and their implication on (chiro)optoelectronic, visco-elastic and mechanical properties (Table 1).

Results and Discussion

All the functionalized NDIs with L-amino acids (L-ANA, L-FNF and L-WNW), D-amino acids (D-ANA, D-FNF and D-WNW) and ethylamine (eNe) were synthesized in single-step reactions (Scheme 1) and characterized by various standard spectroscopic techniques (ESI[†]).¹⁷ Interestingly, we observed that amino acid functionalized NDIs (ANA, FNF and WNW) exhibited ultrasonication assisted room temperature low molecular weight (LMW) gelation property in mixed organic solvent system. The mode of intermolecular interactions and its consequence on properties has been investigated by various spectroscopic and microscopic techniques. Circular dichroism (CD) and X-ray diffraction (XRD) studies revealed the existence of helical ordering of NDIs in both solution and solid state respectively. Photophysical, rheological and microscopy studies revealed unique optoelectronic, visco-elastic and nanoscale ordering properties.

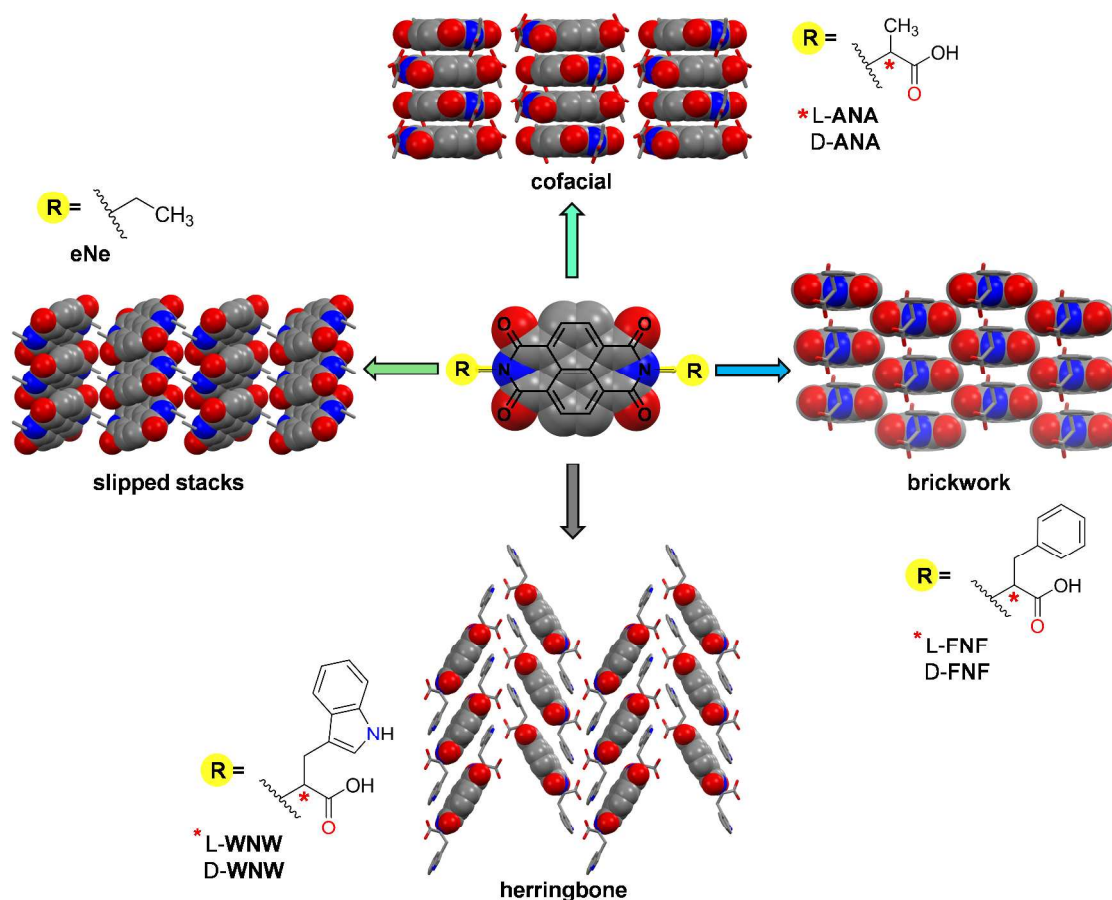


Fig. 1 Single crystal X-ray structures of alanine (L-ANA and D-ANA), phenylalanine (L-FNF and D-FNF), tryptophan (L-WNW and D-WNW) and ethylamine (eNe) functionalized NDIs and their molecular organization into all possible crystal packing modes (cofacial, brickwork, herringbone and slipped stack). The prefix L and D correspond to NDIs functionalized with L-amino acid and D-amino acid respectively. Solvent molecules and hydrogen atoms have been omitted from the crystal packing representation for the clarity.


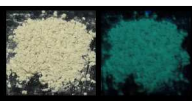

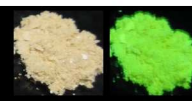
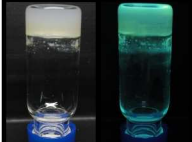
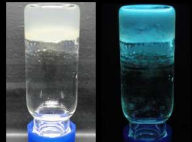

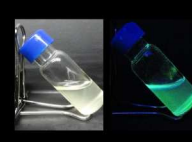

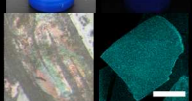

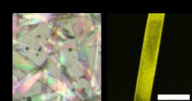
Single crystal XRD studies

We have sought to analyze the solid state packing of NDIs where amino acids and ethyl substituents are used as imide substituents. In particular, the role of structural mutations in the form of amino acid side-chain functionalities and corresponding stereochemistry on the mode of NDI core organization was investigated by single crystal XRD studies. Previous reports have shown slipped stack and brickwork organization of acyclic and cyclic aliphatic imide substituted NDIs respectively.¹⁸ Raymo *et al.* have reported slipped stack packing of glycine functionalized NDI stabilized by solvent induced hydrogen bonding.^{15a} Later, Sanders *et al.* have shown the hydrogen bonded helical nanotube crystal packing using cysteine functionalized NDI with very weak NDI-NDI aromatic interaction.^{13a} Here we describe the systematic molecular programming of NDI by tuning the NDI-NDI aromatic interactions using enantiomeric amino acids with variable α -functionalities. Single crystals of all the compounds (ANA, FNF, WNW and eNe) suitable for X-ray diffraction analysis were grown in a common solvent, dimethyl sulfoxide (DMSO). Alanine (ANA) and ethyl (eNe) functionalized NDIs were found to crystallize in monoclinic crystal system with C_2 and $P2_1/c$ space groups respectively. Aromatic amino acids phenylalanine (FNF) and tryptophan (WNW) conjugated NDIs were

crystallized in orthorhombic crystal system with space groups $C222_1$ and $P2_12_12_1$ respectively. All NDIs exhibited discrete crystal packing from cofacial (ANA), brickwork (FNF), herringbone (WNW) to slipped stacks (eNe) depending the nature of imide substituents as shown in the Fig. 1.

The center of symmetry seemed to play a crucial role in solid state packing of our NDI molecules, especially with respect to aromatic $\pi\cdots\pi$ stacking. There are a few reports documented on this effect in the literature, for example, pyrene crystal structure showed discontinuous $\pi\cdots\pi$ stacks in the form of sandwich herringbone packing, while 2-7-di-tert-butylpyrene-4,5,9,10-tetraone exhibited slipped stacks, both of them putting limits on the extent of $\pi\cdots\pi$ interactions.¹⁹ Among our NDI molecular systems, eNe is centrosymmetric (Fig. S1)¹⁷ and it was observed that the $\pi\cdots\pi$ interactions did not extend in different layers, rather they were found in slipped stack arrangement with limited π -cloud overlap between the adjacent molecules (Fig. 1). To further evaluate the role of center of symmetry, we introduced chirality in the *N*-imide substituents of NDI by functionalization with amino acids. First we studied the effect of L and D alanine as *N*-imide substituents in NDI and the resultant molecules L-ANA and D-ANA respectively exhibited a remarkable cofacial packing with $\pi\cdots\pi$ (NDI \cdots NDI) interactions in columnar fashion (Fig. 1).¹⁷ The crystal structure of ANA revealed non-centrosymmetric

Table 1. Summary of various properties of NDI conjugates^a

Property	ANA	FNF	WNW	eNe
Solid powder				
Gelation				
Crystal				
Supramolecular -ar chirality	enantiopure cofacial columnar stacks	enantiopure supramolecular tilt stacks	enantiopure supramolecular tilt stacks	racemic supramolecular tilt stacks
Optoelec- tronic	Blue-green emission	Cyan emission	Charge transfer interactions	Green emission
Viscoelas- ticity	$G' = 2.22 \times 10^4$ Pa; $\eta_0 = 2.06 \times 10^7$ Pas	$G' = 2.66 \times 10^3$ Pa; $\eta_0 = 2.45 \times 10^6$ Pas	$G' = 1.83 \times 10^4$ Pa; $\eta_0 = 6.72 \times 10^6$ Pas	-
Nanoscale ordering	0D (nano sphere)	1D (nanofiber)	0D (nano sphere)	2D (nano sheet)

^aSacle bar: 200 μ M

structure with distinct columns of $\pi \cdots \pi$ interactions separated by layers of solvent (DMSO) molecules (Fig. S3 and S5).¹⁷ There exist two kinds of alternating NDI-NDI interactions along the column with distances found to be 3.47 Å

5 and 3.56 Å in L-ANA, and 3.48 Å and 3.57 Å in D-ANA. The alternate arrangement is also reflected in the alternate van der Waals (H \cdots H distance 2.27 Å in L-ANA and 2.28 Å in D-ANA) and CH \cdots O (C \cdots O distance 3.07 Å & 3.08 Å in L-ANA and 3.10 Å & 3.08 Å in D-ANA) interactions. However, FNF and WNW with phenylalanine and tryptophan substitutions respectively did not show NDI-NDI cofacial packing. In case of FNF, the NDI core showed layers of brickwork arrangement with effective intermolecular $\pi \cdots \pi$ stacking of phenyl ring and NDI core with the distance of 3.38 Å in L-FNF and 3.46 Å in D-FNF (Fig. 1).¹⁷ The 3D network of FNF lattice was found to be consisted of alternate layers of solvent (DMSO) stabilized by hydrogen bonding between carboxylic acid OH groups and the oxygen atoms of DMSO molecules. The brickwork layers appeared discontinuous due to alternate solvent layers. This discontinuity is clearly observed along *a* and *b* crystallographic axes (Fig. S7 and S9).¹⁷ In case of L-WNW, a relatively small difference in the side-chain of amino acid from phenyl (in FNF) to indole led to the herringbone packing arrangement (Fig. 1). The larger π -electron rich surface of indole (in WNW) as compared to that of

25 phenyl (in FNF) was found to be more effective in inducing strong intermolecular π -electron donor-acceptor (indole-NDI) interactions with reduced interaction distance of 3.20 Å (Fig. S11).¹⁷ Furthermore, additional intermolecular hydrogen bonding interaction of indole-NH with carboxyl oxygen and solvent (DMSO) molecules resulted in confinement of solvent in distinct columns forming solvent channels along the crystallographic *a* axis in the lattice (Fig. S11).¹⁷

It is clear from the above XRD data that only ANA showed twisted cofacial packing with maximum $\pi \cdots \pi$ overlap between NDI cores. The main difference between the molecular arrangement of ANA and other structures lies in the conformation of *C α* substituent with respect to central NDI core. ANA adopted *cis* conformation in which both the side-chain methyl groups of alanine substituents were oriented towards the same side of NDI core. On the other hand, FNF and WNW were stabilized by *trans* conformation where the phenyl and indole groups respectively, were oriented in opposite directions with respect to NDI core.

Photophysical studies

The visible appearance and fluorescence properties of solid powder, organogels and single crystals of NDI conjugates (ANA, FNF, WNW and eNe) under day-light and UV light (365 nm) are shown in Table 1. The intrinsic fluorescence properties of crystals

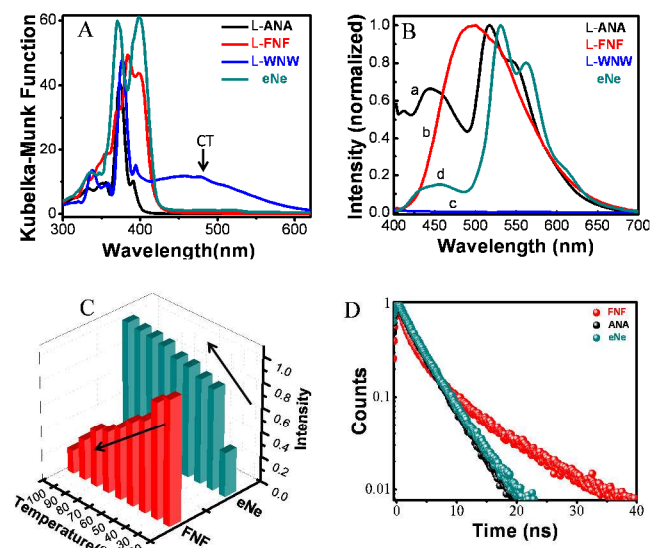


Fig. 2 Transformed UV-vis absorption (A) and fluorescence emission (B) spectra of NDI-conjugates in their solid state. a: L-ANA, b: L-FNF, c: L-WNW and d: eNe. CT: Charge transfer band. (C) TCSPC decay profile of L-ANA ($\lambda_{\text{emission}}$ 552 nm), L-FNF ($\lambda_{\text{emission}}$ 490 nm) and eNe ($\lambda_{\text{emission}}$ 565 nm) with a 405 nm excitation. (D) Temperature versus normalized fluorescence emission intensity of L-FNF (at 490 nm) and eNe (at 563 nm). Absorption spectra (A) were recorded in reflection (R) mode.

were demonstrated by fluorescence microscopy images. The effect of molecular ordering on the optoelectronic properties of NDI was investigated by UV-vis diffused reflectance and fluorescence emission spectroscopy techniques. The diffused reflectance data was transformed into pseudo-absorbance spectra using Kubelka-Munk function (Fig. 2A).¹⁷ The broad NDI absorption bands in the wavelength region of 300–410 nm and 450–550 nm suggesting the presence of strong intermolecular $\pi\cdots\pi$ stacking between the NDI chromophores (Fig. 2A).^{17,20} Notably, the tryptophan appended NDI (WNW) exhibited broad absorption band in the visible region (400–600 nm) attributed to intermolecular through-space, face-centred donor-acceptor charge transfer (CT) interactions between the tryptophan (indole moiety) and NDI chromophore.²⁰ Fluorescence emission spectra of NDI conjugates displayed structureless broad emission bands in the visible spectrum ranging from violet to orange (425 to 650 nm, except WNW) with distinct emission maxima as a consequence of charge delocalization among the different relative orientations of the closely stacked NDI chromophore^{15b} (Fig. 2B).¹⁷ On account of mixture of strong and weak offset π -stacks of NDI-NDI interactions along the inter and intra-layers ANA and eNe exhibited broad (λ_{max} at 450 nm) and longer wavelength emission bands (λ_{max} at 552 and 563 nm respectively).^{11e,12e} FNF displayed a broad excimer-like emission band with λ_{max} at 490 nm.²¹ This is quite remarkable, since most of the unsubstituted and aggregated (solid state) NDIs do not emit in the visible region of the spectrum which makes them unsuitable for fluorescent applications. In the case of WNW, fluorescence emission was quenched completely due to CT interaction, in agreement with the intense CT band observed in the UV-vis absorption spectrum and effective intermolecular indole-NDI interactions in crystal structure (Fig. 2A and Fig. S11).¹⁷ To understand the emission

behaviour of NDI-conjugates, we performed time-correlated single photon counting (TCSPC) experiments with a nanosecond excitation on the solid samples of L-ANA, L-FNF and eNe (Fig. 2C). TCSPC data displayed distinct biexponential decay profiles, which suggest that the observed longer wavelength emission of NDI conjugates is the resultant of two different excitation paths along intra- and inter-layered NDI-NDI interactions as shown in Fig. 1.¹⁷ FNF exhibited significantly longer life-times values (7.23 ns, 36% and 1.63 ns, 64%) as compared to ANA (3.74 ns, 96% and 0.94 ns, 13%) and eNe (1.21 ns, 14% and 3.88 ns, 96%). In addition, the excitation spectra of FNF (monitored at $\lambda_{\text{emission}}$ 490 nm) red-shifted by 15 nm from the absorption band (λ_{max} 398 nm) indicating the existence of preorganized excimer-like aggregates.^{11e,12a,17} Interestingly, the xerogel of FNF and drop-casted film of eNe exhibited temperature responsive emission behaviour as shown in the Fig. 2D.¹⁷ FNF showed gradual quenching of broad emission band at λ_{max} 490 nm with increase in temperature from 20 to 100 °C. In contrast, eNe exhibited enhancement in the 565 nm emission with the rise in temperature. These contrasting temperature responsive emission behaviours are attributed to thermal disruption of intermolecular aromatic complexation between phenyl and NDI core in FNF and formation of emissive dimeric form of eNe.²¹ Therefore, the xerogel of FNF and drop-casted film of eNe can be used as solid state temperature sensor systems.

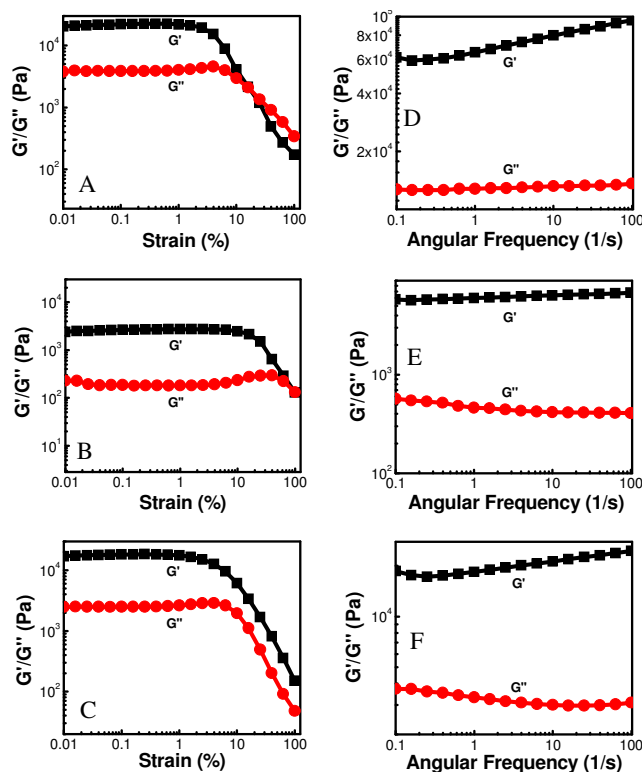


Fig. 3 Rheological studies of organogels of amino acid-NDI conjugates. Stress sweep experiments (A–C) and frequency sweep experiments (D–F) of ANA (A and D), FNF (B and E) and WNW (C and F) respectively. G' : storage modulus (■) and G'' : loss modulus (●)

Rheological studies

All amino acid-NDI conjugates showed ultrasonication induced gelation property in mixed organic solvent systems. Here we have selected CHCl_3 (for **FNF**) and tetrahydrofuran (THF) (for **ANA** and **WNW**) as good solvents and nonpolar methylcyclohexane (MCH) was slowly added to induce gelation through effective $\pi\cdots\pi$ stacking and hydrogen bonding between the molecules (concentration used for gelation was 6 mM and MCH/good solvent: 80/20 v/v). Surprisingly, racemic mixtures of amino acid-NDI conjugates (1:1 mixtures of L and D isomers of **ANA/FNF/WNW**) and achiral **eNe** did not undergo gelation under similar conditions. We further investigated the influence of $\text{C}\alpha$ -functionalities on mechanical properties of organogels by dynamic rheology studies. The amplitude sweep and frequency sweep experiments at 20 °C displayed greater storage modulus (G') than loss modulus (G'') within the linear visco-elastic region (Fig. 3). These results revealed the presence of a typical soft solid-like gel-phase in organogels of all the amino acid-NDI conjugates. The storage modulus G' and loss modulus G'' associated with the energy storage and loss of energy respectively were measured at 20 °C as functions of shear stress (stress sweep) at a constant frequency of 1.6 Hz (Fig. 3A-C). The recorded G' was found to be maximum in case of **ANA** (2.22×10^4 Pa, Fig. 3A) and minimum for **FNF** (2.66×10^3 Pa, Fig. 3B) gels respectively, whereas that of **WNW** gel was found to be 1.83×10^4 Pa (Fig. 3C). Amusingly, **WNW** gel did not show crossover of G' and G'' under the given stress sweep, indicating excellent energy storage property. **ANA** and **FNF** displayed crossover of G' and G'' at 15.9% and 99.9% strain values respectively. The observed good storage property of **WNW** compared to **ANA** and **FNF** may be attributed to the presence of strong donor-acceptor CT $\pi\cdots\pi$ interactions and additional indole-NH hydrogen bonding among its molecules and with the solvent.

To understand the consequence of various noncovalent interactions on the tolerance of the gel upon exposure to external forces, an angle frequency sweep experiment was conducted within the gels linear visco-elastic region (Fig. 3D-F). The results showed higher storage modulus (G') than the loss modulus (G'') due to the absence of phase separation or phase transition during the sweep process. Furthermore, both G' and G'' remained relatively stable within the whole frequency range indicating that the gel possessed an excellent tolerance to external forces. The property of material to avoid sedimentation upon storage was determined by calculating the zero shear viscosity (η_0) and the values were found to be 2.06×10^7 Pa.s (**ANA**) $>$ 6.72×10^6 Pa.s (**WNW**) $>$ 2.45×10^6 Pa.s (**FNF**). Rheological studies (both stress sweep and frequency sweep) revealed the ability of tuning the mechanical strength and elasticity of NDI organogels by ingenious noncovalent interactions drive molecular organization induced through amino acid side-chain functionality.

CD studies

In order to probe the effect of enantiomeric amino acids on the chiroptical properties of achiral NDI chromophore organization, we have performed CD studies in both crystal and gel forming solvent systems I) MCH/THF:80:20, v/v, II) DMSO and III) MCH/ CHCl_3 :80/20, v/v (Fig. 4). All the enantiomeric amino acid conjugates, L-**ANA** and D-**ANA** (Fig. 4A), L-**FNF** and D-**FNF**

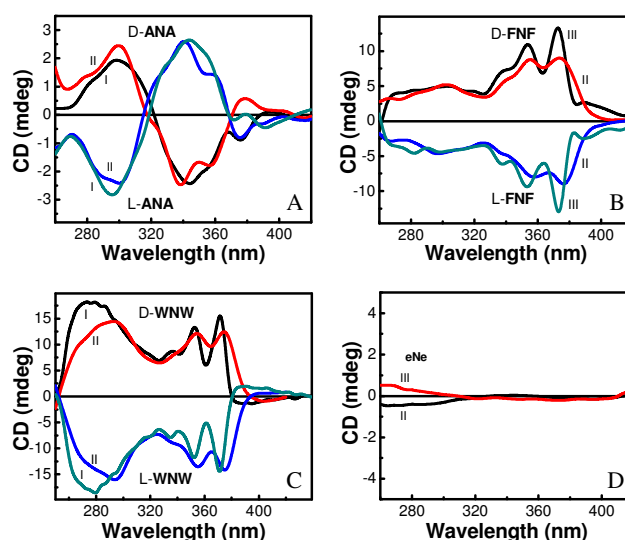


Fig. 4 CD spectra of L- and D-isomers of A) **ANA**, B) **FNF**, C) **WNW** and D) **eNe** in gelling solvents (I: MCH/THF and III: MCH/ CHCl_3) and crystal forming solvent (II: DMSO).

(Fig. 4B) and L-**WNW** and D-**WNW** (Fig. 4C) exhibited mirror image Cotton effects in the NDI absorption region (250-400 nm) ascribed to the presence of chiral intermolecular assembly of NDI molecules.^{12,15} The positive (*D-isomer) and negative (*L-isomer) Cotton effects are attributed to differential absorption of circularly polarized light by right handed (P-type) and left handed (M-type) supramolecular helical organization of NDI chromophores respectively. Whereas, in case of **eNe**, a flat CD signal was observed due to its symmetrical (centrosymmetric) structure and the absence of chiral center in the imide-substituents (Fig. 4D). This confirmed the formation of supramolecular chiral aggregates via transcription of chiral information from the α -stereocentre of N-imide amino acid substituents to central achiral NDI chromophoric unit.^{4i, 12-13} The difference in the shape and amplitude of CD signals for NDI-conjugates with variable amino acid substituents suggested distinct inter-chromophoric distances, projection angles and number of interacting NDI-chromophores.^{13b}

Solid state molecular helical organization studies

To corroborate the CD results discussed above, we further investigated the solid state chirality in crystal packing. Several organic molecules exhibit 2 fold helices in solid state packing by the virtue of presence of 2_1 screw axes in the crystal lattice.^{19,22} L-**ANA** and D-**ANA** exhibited cofacial helical columnar stacks with a twist of 69.17° (anticlockwise) and 69.27° (clockwise) respectively between successive molecules (Fig. 5A,B). This twist is due to the steric hindrance as well as hydrogen bond potential of alanine residues (-COOH group) on both sides of the NDI core with solvent (DMSO) (Fig. S3 and S5). In contrast, **FNF** and **WNW** displayed supramolecular tilt helical organization of molecules with respect to 2_1 screw axis. Hisaki *et al.*²² have reported a method to distinguish between right and left handed supramolecular tilt chirality of such twofold helical assemblies. Based on this method, we correlated the organization of aromatic amino acid-NDI conjugate with the supramolecular

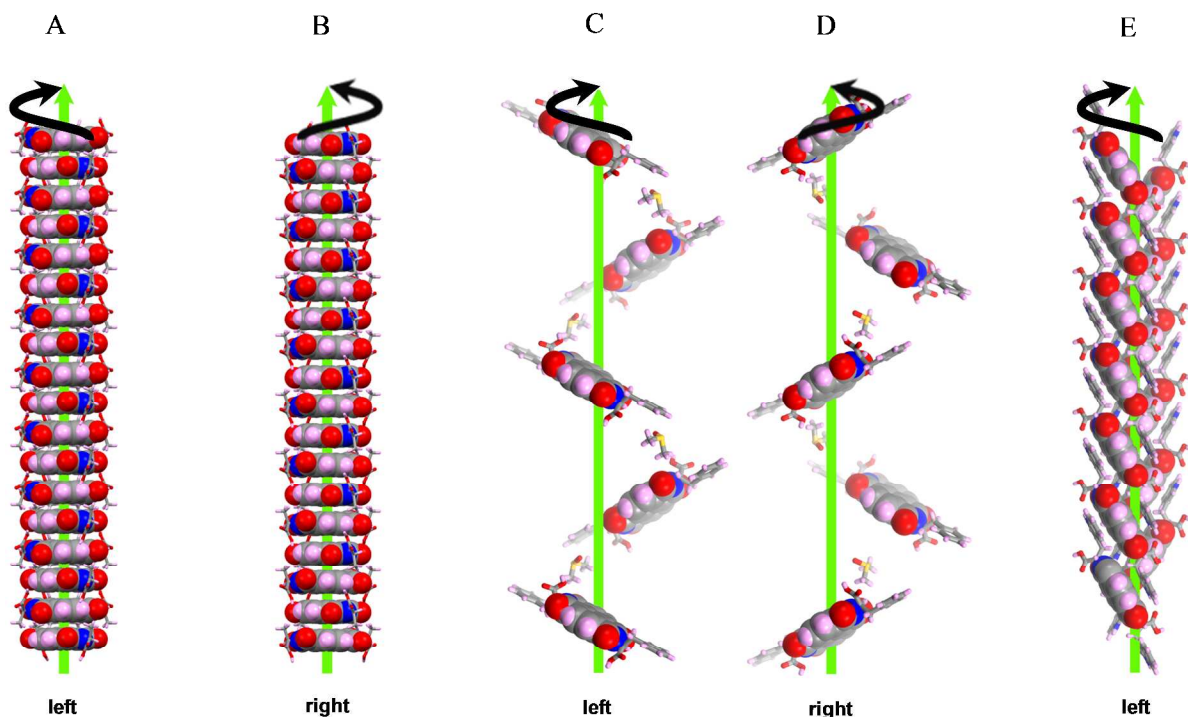


Fig. 5 Solid state helical organization of A) L-ANA , B) D-ANA , C) L-FNF, D) D-FNF and E) L-WNW in their respective crystal lattice. (A and B) cofacial helical columnar stacks and (C-E) supramolecular tilt helical organization.

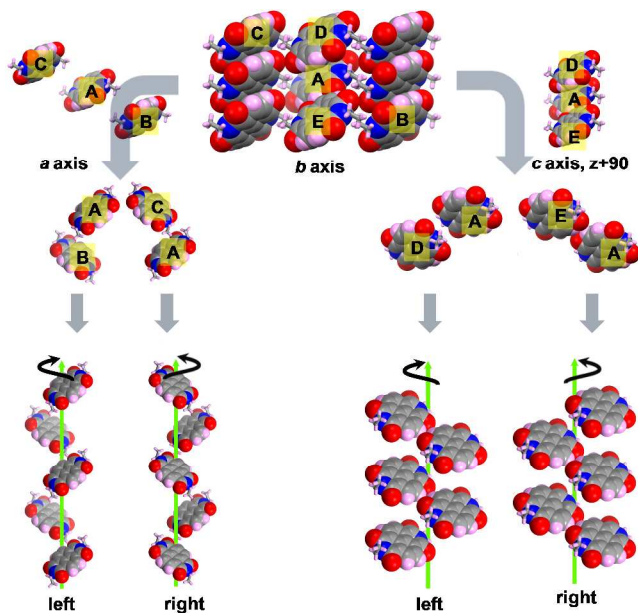


Fig. 6 The 2_1 helicity inherent in the eNe $P2_1/c$ crystal system. Four helices embedded within the crystal lattice: side-to-side enantiomeric pairs AB (left handed) and AC (right handed) along the crystallographic c axis and slipped herringbone enantiomeric pairs AD (left handed) and AE (right handed) along crystallographic a axis.

tilt chirality. L-FNF and L-WNW showed left handed supramolecular tilt chirality whereas D-FNF showed right handed helical assemblies (Fig. 5C-E). Our effort in crystallizing D-WNW was not fruitful, nevertheless CD data in Fig. 4 strongly suggests right handed helical arrangement in solid state. The centrosymmetric eNe showed coexisting left and right handed helical assemblies in the crystal lattice (Fig. 6) as expected from its racemic nature revealed by the flat CD signals as shown in Fig. 4D.

The three parameters, viz. pitch, tilt and the distance of centroid of the molecule from the helix axis were calculated to define the 2_1 helices. In various conjugates, the helices were considered along different directions based on the arrangement of molecules in their respective crystal lattices. FNF showed prominent 2_1 helix along the crystallographic c axis with tilt angle of 66.09° for L-FNF and 66.15° for D-FNF, and the centroid of each molecule is 3.14 \AA from the center of the helix. The pitch of the helix was found to be 27.66 \AA and 28.20 \AA in L-FNF and D-FNF respectively (Fig. S7 and S9).¹⁷ These helices were found to be stabilized by interactions of DMSO (solvent) methyl groups with C α atom of the amino acid (van der Waals interaction) and phenyl ring through CH \cdots π interaction. (Fig. S7 and S9).¹⁷ WNW crystallized in $P2_12_12_1$ space group with three mutually perpendicular 2_1 screw axes. However, only two of them, viz. a and b crystallographic axis displayed supramolecular helices with tilt chirality. The 2_1 helix along a -axis was considered for determination of various parameters of WNW (Fig. S11).¹⁷ Here the tilt angle was 115.64° , the centroid to helix axis distance was 3.93 \AA and the pitch of the helix was 8.67 \AA . As shown by Hisaki

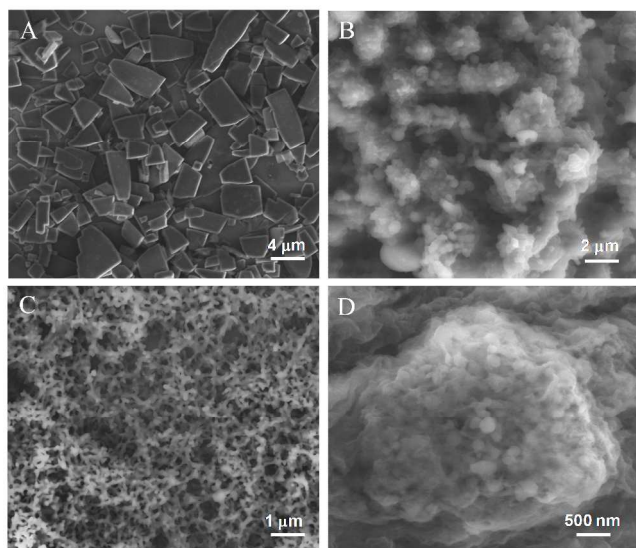


Fig. 7 FESEM micrographs of A) drop casted **eNe** solution (MCH/CHCl₃: 80/20 V/V), and xerogels of B) **ANA**, C) **FNF**, and D) **WNW**.

*et al.*²² the adjacent 2₁ helices of **WNW** were antiparallel (Fig. S11).¹⁷ Two types of CH...O interactions and CT π ... π stacking were found to stabilize these antiparallel helices. One of them was observed between indole CH group and imide carbonyl oxygen of NDI core, while the other was found between carboxylic acid oxygen and aromatic CH of NDI core. The 2₁ helicity inherent in the **eNe** P2₁/c crystal system was analyzed using a reported method.^{22a} On the basis of this method, we have observed four helices embedded within the crystal lattice (Fig. 6). Two of them *viz.* AB (left handed) and AC (right handed), were found to be arranged as side-to-side enantiomeric pairs along the crystallographic *c* axis and the other two *viz.* AD (left handed) and AE (right handed) as slipped herringbone packing along *a* axis. The tilt angle of helices was about 44.63° and centroid to helix axis distance was found to be 3.11 Å. Therefore the observed CD inactiveness of **eNe** (Fig. 4D) was attributed to equal propensity for supramolecular organization of centrosymmetric molecules into left and right handed helices.

Morphological studies of xerogels

The effect of structural mutations on the morphologies of self-assembled structures of NDI from the solution upon drop casting or in the organogels was examined by field emission scanning electron microscopy (FESEM). FESEM samples were prepared by drop casting the solution of **eNe** onto the silicon wafer and dried at room temperature and vacuum. The xerogel samples were prepared by transferring the organogels onto the silicon wafer followed by vacuum drying. Remarkably, FESEM micrographs revealed interesting 0D, 1D and 2D morphological structures (Fig. 7). The **eNe** self-assembled from its solution (MCH/CHCl₃: 80/20, v/v) into large surface area 2D nano and mesosheets with several micrometer lateral dimensions (Fig. 7A). In contrast, the xerogels of amino acid-NDI conjugates revealed the presence of distinct 0D and 1D nanostructures. **ANA** (Fig. 7B) and **WNW** (Fig. 7D)¹⁷ xerogels' matrix displayed embedded nanospheres with diameter of 100 to 300 nm (**ANA**) and 50 to 500 nm (**WNW**) respectively. **FNF** showed remarkable 3D

network of interconnected high aspect ratio 1D nanofibers responsible for the observed gelation (Fig. 7C).¹⁷ The fibers were several micrometers in length and 20 to 100 nm in diameter. The observed 2D, 1D and 0D nanostructures of NDI are ascribed to various intermolecular noncovalent interactions (hydrogen bonding, π ... π , van der Waals, CH... π , and CH...O) induced by side chain functionalities. These results clearly supported the potential of minute structural mutations in the imide substitution in fine tuning the nanoscale molecular ordering of NDIs.

Conclusions

In conclusion, for the first time we have demonstrated engineering of most promising NDI-NDI aromatic molecular ordering into all possible packing modes namely cofacial, brickwork, herringbone and slipped stacks using biomimetic approach in solid state. The center of symmetry, the structural mutations (C α substituents on amino acids), corresponding chirality and their conformations with respect to planar NDI core were found to have major influence on the solid state molecular organization. Photophysical studies showed remarkable influence of molecular ordering on the absorption and emission properties of NDIs. Interestingly, NDI conjugates showed solid state emission in visible region from violet to orange, promising as potential materials for fluorescence applications. **WNW** exhibited strong absorption in entire visible region with the quenching of fluorescence due to effective charge transfer between indole (tryptophan) ring and NDI core making it a potential candidate for photovoltaic applications. All amino acid-NDI conjugates formed ultrasonication induced organogels and their rheological data revealed tunable visco-elastic ability with promising storage property. Furthermore, xerogel of **FNF** and drop-casted film of **eNe** exhibited contrasting temperature responsive emission behaviors and they can be used as solid state temperature sensor systems. The transcription of chiral information from amino acids to achiral NDI core was demonstrated by the preferential chiral helical arrangement of molecules. Whereas achiral ethyl substituents in NDI led to coexistence of both left and right handed helical (racemic mixture) arrangement of molecules. **ANA** with aliphatic amino acid (alanine) resulted in cofacial helical columnar stack, whereas **FNF** and **WNW** with aromatic amino acids (phenylalanine and tryptophan respectively) exhibited supramolecular tilt chirality. We were also successful in tuning the nanoscale supramolecular assembly of NDIs into 0D nanospheres (**ANA** and **WNW**), 1D nanofibers (**FNF**) and 2D sheets (**eNe**). Overall, the structural mutations (amino acids) are capable of inducing preferential helical bias and tunable molecular ordering which in turn give rise to interesting optical (for example solid state emission, charge transfer) and viscoelastic (for example gelation and mechanical properties) and distinct nanoscale ordering properties to NDI system. We believe that our novel biomimetic design strategy is highly useful in understanding and mimicking the Nature's complex molecular interactions and fine-tuning of aromatic functional properties for future electronics, chiroptical and biomedical applications.

Acknowledgements

Authors thank Prof. C. N. R. Rao for constant support and encouragement, JNCASR, Department of Biotechnology (DBT)-Innovative Young Biotechnologist Award (IYBA) (Grant BT/03/IYBA/2010), India for financial support, H.K. for CSIR fellowship, Anton Paar India Pvt. Ltd., Bangalore, for rheological measurements.

Notes and references

^a *Biorganic Chemistry Laboratory, New Chemistry Unit, Jawaharlal Nehru Centre for Advanced Scientific Research, Jakkur P.O., Bangalore 560064, India. Fax: (+) 91 80 22082627; E-mail: tgraju@jncasr.ac.in*

^b *Department of Physics, Indian Institute of Science, Bangalore-560012, India.*

† Electronic Supplementary Information (ESI) available: [Synthetic procedure, characterization and Crystallographic information]. See DOI: 10.1039/b000000x/

‡ Crystal structure determination

eNe: C₁₈H₁₄N₂O₄, *M* = 322.31, monoclinic, *a* = 4.8667(3), *b* = 7.7561(4), *c* = 18.3813(12) Å, β = 90.214(4)°, *U* = 693.83(7) Å³, *T* = 100 K, space group *P*2₁/*c* (no.14), *Z* = 2, 7958 reflections measured, 1863 unique (*R*_{int} = 0.0361) which were used in all calculations. The final *wR*(*F*₂) was 0.1257 (all data). CCDC 937648.

L-FNF: C₃₆H₃₄N₂O₁₀S₂, *M* = 718.77, orthorhombic, *a* = 8.953(3), *b* = 13.508(6), *c* = 27.663(11) Å, *U* = 3345(2) Å³, *T* = 100 K, space group *C*222₁ (no.20), *Z* = 4, 8522 reflections measured, 1223 unique (*R*_{int} = 0.1165) which were used in all calculations. The final *wR*(*F*₂) was 0.2233 (all data). CCDC 937649.

D-FNF: C₃₆H₃₄N₂O₁₀S₂, *M* = 718.77, orthorhombic, *a* = 9.104(7), *b* = 13.550(10), *c* = 28.20(2) Å, *U* = 3479(4) Å³, *T* = 100 K, space group *C*222₁ (no.20), *Z* = 4, 5069 reflections measured, 1123 unique (*R*_{int} = 0.1052) which were used in all calculations. The final *wR*(*F*₂) was 0.2050 (all data). CCDC 937650.

L-WNW: C₄₂H₄₂N₄O₁₃S₃, *M* = 909.41, orthorhombic, *a* = 8.670(2), *b* = 19.624(5), *c* = 25.099(7) Å, *U* = 4270.4(19) Å³, *T* = 100 K, space group *P*2₁2₁2₁ (no.19), *Z* = 4, 12276 reflections measured, 4916 unique (*R*_{int} = 0.1372) which were used in all calculations. The final *wR*(*F*₂) was 0.1685 (all data). CCDC 937651.

L-ANA: C₂₄H₂₆N₂O₁₀S₂, *M* = 566.59, monoclinic, *a* = 24.2349(5), *b* = 7.02890(10), *c* = 14.7664(3) Å, β = 90.8260(10)°, *U* = 2515.12(8) Å³, *T* = 100 K, space group *C*2 (no.5), *Z* = 4, 47595 reflections measured, 4150 unique (*R*_{int} = 0.0506) which were used in all calculations. The final *wR*(*F*₂) was 0.0887 (all data). CCDC 937652.

D-ANA: C₂₄H₂₆N₂O₁₀S₂, *M* = 566.59, monoclinic, *a* = 24.302(2), *b* = 7.0441(6), *c* = 14.8026(11) Å, β = 90.782(5)°, *U* = 2533.7(4) Å³, *T* = 100 K, space group *C*2 (no.5), *Z* = 4, 9893 reflections measured, 4100 unique (*R*_{int} = 0.0482) which were used in all calculations. The final *wR*(*F*₂) was 0.0966 (all data). CCDC 937653.

The supplementary crystallographic data for this paper can be obtained from the Cambridge Crystallographic Data Centre (CCDC) via www.ccdc.cam.ac.uk/data_request/cif.

- (1) (a) S. K. Burley and G. A. Petsko, *Science*, 1985, **229**, 23-28. (b) C. A. Hunter, *Phil. Trans. R. Soc. Lond.*, 1993, **345**, 77-85. (c) E. Gazit, *The FASEB Journal*, 2002, **16**, 77-83. (d) L. M. Salonen, M. Ellermann and F. Diederich, *Angew. Chem. Int. Ed.*, 2011, **50**, 4808-4842. (e) K. E. Riley and P. Hobza, *Acc. Chem. Res.*, 2013, **46**, 927-936.
- (2) (a) M. A. Cejas, W. A. Kinney, C. Chen, G. C. Leo, Tounge, B. A. J. G. Vinter, P. P. Joshi and B. E. Maryanoff, *J. Am. Chem. Soc.*, 2007, **129**, 2202-2203. (b) L. Zang, Y. Che and J. S. Moore, *Acc. Chem. Res.*, 2008, **41**, 1596-1608. (c) C. J. Bowerman, W. Liyanage, A. J. Federation and B. L. Nilsson, *Biomacromolecules*, 2011, **12**, 2735-2745. (d) T. Aida, E. W. Meijer and S. I. Stupp, *Science*, 2012, **335**, 813-817. (e) M. B. Avinash and T. Govindaraju, *Adv. Mater.*, 2012, **24**, 3905-3922. (f) J. S. Meisner, D. F. Sedbrook, M. Krikorian, J. Chen, A. Sattler, M. E. Carnes, C. B. Murray, M. Steigerwald and C. Nuckolls, *Chem. Sci.*, 2012, **3**, 1007-1014. (g) A. C. Fahrenbach, S. C. Warren, J. T. Inorvati, A.-J. Avestro, J. C. Barnes, J. F. Stoddart and B. A. Grzybowski, *Adv. Mater.*, 2013, **25**, 331-348.

- (3) (a) C. A. Hunter and J. K. M. Sanders, *J. Am. Chem. Soc.*, 1990, **112**, 5525-5534. (b) S. E. Wheeler, *J. Am. Chem. Soc.*, 2011, **133**, 10262-10274. (c) D. Yan, A. Delori, G. O. Lloyd, T. Friščić, G. M. Day, W. Jones, J. Lu, M. Wei, D. G. Evans, and X. Duan, *Angew. Chem. Int. Ed.*, 2011, **50**, 12483-12486. (d) C. R. Martinez and B. L. Iverson, *Chem. Sci.*, 2012, **3**, 2191-2201. (e) J. Stojaković, A. M. Whitis and L. R. MacGillivray, *Angew. Chem. Int. Ed.*, 2013, **46**, 12127-12130.
- (4) (a) H. Ogoshi and T. Mizutani, *Acc. Chem. Res.*, 1998, **31**, 81-89. (b) B. L. Feringa, R. A. van Delden, N. Koumura and E. M. Geertsema, *Chem. Rev.*, 2000, **100**, 1789-1816. (c) J. Zhang, M. T. Albelda, Y. Liu and J. W. Canary, *Chirality*, 2005, **17**, 404-420. (d) G. A. Hembury, V. V. Borovkov and Y. Inoue, *Chem. Rev.*, 2007, **108**, 1-73. (e) T. Yamamoto, T. Yamada, Y. Nagata and M. Sugimoto, *J. Am. Chem. Soc.*, 2010, **132**, 7899-7901. (f) B. M. Rosen, M. Peterca, K. Morimitsu, A. S. E. Dulcey, P. Leowanawat, A.-M. Resmerita, M. R. Imam and V. Percec, *J. Am. Chem. Soc.*, 2011, **133**, 5135-5151. (g) J.-M. Suk, V. R. Naidu, X. Liu, M. S. Lah and K.-S. Jeong, *J. Am. Chem. Soc.*, 2011, **133**, 13938-13941. (h) Z. Dai, J. Lee and W. Zhang, *Molecules*, 2012, **17**, 1247-1277. (i) M. Pandeeswar, M. B. Avinash and T. Govindaraju, *Chem. Eur. J.*, 2012, **18**, 4818-4822. (j) A. Gopal, M. Hifudheen, S. Furumi, M. Takeuchi and A. Ajayaghosh, *Angew. Chem. Int. Ed.*, 2012, **51**, 10505-10509.
- (5) (a) M. M. Green, M. P. Reidy, R. D. Johnson, G. Darling, D. J. O'Leary and G. Willson, *J. Am. Chem. Soc.*, 1989, **111**, 6452-6454. (b) R. H. Martin, *Angew. Chem. Int. Ed. Engl.*, 1974, **13**, 649-660. (c) A. E. Rowan and R. J. M. Nolte, *Angew. Chem. Int. Ed.*, 1998, **37**, 63-68. (d) V. Berl, I. Huc, R. G. Khoury and J.-M. Lehn, *Chem. Eur. J.*, 2001, **7**, 2810-2820. (e) C. Schmuck, *Angew. Chem. Int. Ed.*, 2003, **42**, 2448-2452. (f) M. A. Mateos-Timoneda, M. Crego-Calama and D. N. Reinhoudt, *Chem. Soc. Rev.*, 2004, **33**, 363-372. (g) E. Ohta, H. Sato, S. Ando, A. Kosaka, T. Fukushima, D. Hashizume, M. Yamasaki, K. Hasegawa, A. Muraoka, H. Ushiyama, K. Yamashita, and T. Aida, *Nat. Chem.*, 2011, **3**, 68-73. (h) K. Watanabe, K. Suda and K. Akagi, *J. Mater. Chem. C*, 2013, **1**, 2797-2805. (i) Y. Yang, Y. Zhang and Z. Wei, *Adv. Mater.*, 2013, **42**, 6039-6049.
- (6) (a) A. R. A. Palmans and E. W. Meijer, *Angew. Chem. Int. Ed.*, 2007, **46**, 8948-8968. (b) V. K. Praveen, S. S. Babu, C. Vijayakumar, R. Varghese and A. Ajayaghosh, *Bull. Chem. Soc. Jpn.*, 2008, **81**, 1196-1211. (c) B. M. Rosen, C. J. Wilson, D. A. Wilson, M. Peterca, M. R. Imam and V. Percec, *Chem. Rev.*, 2009, **109**, 6275-6540. (d) D. Chakrabarti, S. N. Fejer and D. J. Wales, *Pro. Natl Acad. Sci. USA*, 2009, **106**, 20164-20167. (e) E. Yashima, K. Maeda, H. Iida, Y. Furusho and K. Nagai, *Chem. Rev.*, 2009, **109**, 6102-6211. (f) M. M. Safont-Sempere, P. Osswald, M. Stolte, M. Grune, M. Renz, M. Kaupp, K. Radacki, H. Braunschweig and F. Wurthner, *J. Am. Chem. Soc.*, 2011, **133**, 9580-9591. (g) F. Freire, J. M. Seco, E. Quiñoa and R. Riguera, *Angew. Chem. Int. Ed.*, 2011, **50**, 11692-11696. (h) Y. Nagata, T. Yamada, T. Adachi, Y. Akai, T. Yamamoto and M. Sugimoto, *J. Am. Chem. Soc.*, 2013, **135**, 10104-10113. (i) S. T. Schneckel, M. Frascioni, Z. Liu, Y. Wu, D. M. Gardner, N. L. Strutt, C. Cheng, R. Carmieli, M. R. Wasielewski and J. F. Stoddart, *Angew. Chem. Int. Ed.*, 2013, **52**, 13100-13104.
- (7) (a) D. Adam, P. Schuhmacher, J. Simmerer, L. Häussling, K. Siemensmeyer, K. H. Etbachi, H. Ringsdorf and D. Haarer, *Nature*, 1994, **371**, 141-143. (b) V. Percec, M. Glodde, T. K. Bera, Y. Miura, I. Shiyonovskaya, K. D. Singer, V. S. K. Balagurusamy, P. A. Heiney, I. Schnell, A. Rapp, H. W. Spiess, S. D. Hudson and C. Duan, *Nature*, 2002, **417**, 384-387. (c) L. M. Herz, C. Daniel, C. Silva, F. J. M. Hoeben, A. P. H. J. Schenning, E. W. Meijer, R. H. Friend and R. T. Phillips, *Phys. Rev. B*, 2003, **68**, 045203.
- (8) (a) D. B. Amabilino and J. Puigmarti-Luis, *Soft Matter*, 2010, **6**, 1605-1612. (b) S. S. Babu, S. Prasanthkumar, A. Ajayaghosh, *Angew. Chem. Int. Ed.*, 2012, **51**, 1766-1776.
- (9) (a) J. E. Anthony, *Chem. Rev.*, 2006, **106**, 5028-5048. (b) M.; Mas-Torrent and C. Rovira, *Chem. Rev.*, 2011, **111**, 4833-4856. (c) C. Wang, H. Dong, W. Hu, Y. Liu and D. Zhu, *Chem. Rev.*, 2012, **112**, 2208-2267. (d) S. Ghosh and C. M. Reddy, *Angew. Chem. Int. Ed.*, 2012, **51**, 10319-10323.
- (10) (a) J. E. Anthony, A. Facchetti, M. Heeney, S. R. Marder and X. Zhan, *Adv. Mater.*, 2010, **22**, 3876-3892. (b) T. Weil, T. Vosch, J. Hofkens, K. Peneva and K. Müllen, *Angew. Chem. Int. Ed.*, 2010, **49**,

- 9068-9093. (c) F. Wurthner and M. Stolte, *Chem. Commun.*, 2011, **47**, 5109-5115. (e) X. Zhan, A. Facchetti, S. Barlow, T. J. Marks, M. A. Ratner, M. R. Wasielewski and S. R. Marder, *Adv. Mater.*, 2011, **23**, 268-284.
- 5 (11) (a) S. V. Bhosale, C. H. Jani and S. J. Langford, *Chem. Soc. Rev.*, 2008, **37**, 331-342. (b) V. Tumiatti, A. Milelli, A. Minarini, M. Micco, A. Gasperi Campani, L. Roncuzzi, D. Baiocchi, J. Marinello, G. Capranico, M. Zini, C. Stefanelli, C. Melchiorre, *J. Med. Chem.*, 2009, **52**, 7873-7877. (c) Y. Takashima, V. M. Martinez, S. Furukawa, M. Kondo, S. Shimomura, H. Uehara, M. Nakahama, K. Sugimoto and S. Kitagawa, *Nature Commun.*, 2010, **2**, 168. (d) S. Guha, F. S. Goodson, L. J. Corson and S. Saha, *J. Am. Chem. Soc.*, 2012, **134**, 13679-13691. (e) J. B. Bodapati and H. Icil, *Photochem. Photobiol. Sci.*, 2011, **10**, 1283-1293. (f) M. R. Molla and S. Ghosh, *Chem. Eur. J.*, 2012, **18**, 1290-1294. (g) S. V. Bhosale, S. V. Bhosale and S. K. Bhargava, *Org. Biomol. Chem.*, 2012, **10**, 6455-6468. (h) N. Narayanaswamy, M. B. Avinash and T. Govindaraju, *New J. Chem.*, 2013, **37**, 1302-1306. (i) A. Takai, T. Yasuda, T. Ishizuka, T. Kojima and M. Takeuchi, *Angew. Chem. Int. Ed.*, 2013, **52**, 9167-9171.
- 10 (12) (a) H. Shao, T. Nguyen, N. C. Romano, D. A. Modarelli and J. R. Parquette, *J. Am. Chem. Soc.*, 2009, **131**, 16374-16376. (b) H. Shao, J. Seifert, N. C. Romano, M. Gao, J. J. Helmus, C. P. Jaronec, D. A. Modarelli and J. R. Parquette, *Angew. Chem. Int. Ed.*, 2010, **49**, 7688-7691. (c) H. Shao, M. Gao, S. H. Kim, C. P. Jaronec and J. R. Parquette, *Chem. Eur. J.*, 2011, **17**, 12882-12885. (d) S. Manchineella, V. Prathyusha, U. Deva Priyakumar, and T. Govindaraju, *Chem. Eur. J.*, 2013, **19**, 16615-16624. (e) M. R. Molla, D. Gehrig, L. Roy, V. Kamm, A. Paul, F. Laquai and S. Ghosh, *Chem. Eur. J.*, 2014, **20**, 760-771.
- 15 (13) (a) G. D. Pantoş, P. Pengo and J. K. M. Sanders, *Angew. Chem. Int. Ed.*, 2007, **46**, 194-197. (b) B. M. Bulheller, G. D. Pantos, J. K. M. Sanders and J. D. Hirst, *Phys. Chem. Chem. Phys.*, 2009, **11**, 6060-6065. (c) T. W. Anderson, J. K. M. Sanders, G. D. Pantos, *Org. Biomol. Chem.*, 2010, **8**, 4274-4280. (d) N. Ponnuswamy, G. D. Pantos, M. M. J. Smulders and J. K. M. Sanders, *J. Am. Chem. Soc.*, 2012, **134**, 566-573. (e) K. Tambara, J.-C. Olsen, D. E. Hansen and G. D. Pantos, *Org. Biomol. Chem.*, 2014, **12**, 607-614.
- 20 (14) (a) S. Bhosale, A. L. Sisson, P. Talukdar, A. Furstenberg, N. Banerji, E. Vauthey, G. Bollot, J. Mareda, C. Roger, F. Wurthner, N. Sakai and S. Matile, *Science*, 2006, **313**, 84-86. (b) R. Bhosale, J. Misek, N. Sakai and S. Matile, *Chem. Soc. Rev.*, 2010, **39**, 138-149.
- 25 (15) (a) M. Tomasulo, D. M. Naistat, A. J. P. White, D. J. Williams and F. M. Raymo, *Tetrahedron Lett.*, 2005, **46**, 5695-5698. (b) N. Ashkenasy, W. S. Horne and M. R. Ghadiri, *Small*, 2006, **2**, 99-102. (c) M. B. Avinash and T. Govindaraju, *Nanoscale*, 2011, **3**, 2536-2543.
- 30 (16) (a) A. C. Bhasikuttan, J. Mohanty, W. M. Nau and H. Pal, *Angew. Chem. Int. Ed.* **2007**, *119*, 4198-4200. (b) A. Jatsch, E. K. Schillinger, S. Schmid and P. Bauerle, *J. Mater. Chem.*, 2010, **20**, 3563-3578. (c) R. i. M. Owens and G. G. Malliaras, *MRS Bulletin*, 2010, **35**, 449-456. (d) S. H. Kim and J. R. Parquette, *Nanoscale*, 2012, **4**, 6940-6947. (e) S. Sengupta and F. Wurthner, *Acc. Chem. Res.*, 2013, **46**, 2458-2512. (f) J. D. Tovar, *Acc. Chem. Res.*, 2013, **46**, 1527-1537.
- 35 (17) Electronic supporting information (ESI).
- 40 (18) (a) P. M. Alvey, J. J. Reczek, V. Lynch and B. L. Iverson, *J. Org. Chem.*, 2010, **75**, 7682-7690. (b) T. Kakinuma, H. Kojima, M. Ashizawa, H. Matsumoto and T. Mori, *J. Mater. Chem. C*, 2013, **1**, 5395-5401.
- 45 (19) (a) C. S. Frampton, K. S. Knight, N. Shankland and K. Shankland, *J. Mol. Struct.*, 2000, **520**, 29-32. (b) Z. Wang, V. Enkelmann, F. Negri and K. Müllen, *Angew. Chem. Int. Ed.*, 2004, **43**, 1972-1975. (c) K. Kobayashi, R. Shimaoka, M. Kawahata, M. Yamanaka and K. Yamaguchi, *Org. Lett.*, 2006, **8**, 2385-2388.
- 50 (20) (a) P. Mukhopadhyay, Y. Iwashita, M. Shirakawa, S.-i. Kawano, N. Fujita and S. Shinkai, *Angew. Chem. Int. Ed.* 2006, **45**, 1592-1595. (b) Y. Ofir, A. Zelichenok and S. Yitzchaik, *J. Mater. Chem.*, 2006, **16**, 2142-2149. (c) P. Ganesan, B. van Lagen, A. T. M. Marcelis, E. J. R. Sudholter and H. Zuilhof, *Org. Lett.*, 2007, **9**, 2297-2300. (d) K. Liu, Y. Yao, Y. Liu, C. Wang, Z. Li and X. Zhang, *Langmuir* 2012,
- 55 **28**, 10697-10702. (e) B. D. McCarthy, E. R. Hontz, S. R. Yost, T. Van Voorhis and M. Dincă, *J. Phys. Chem. Lett.*, 2013, **4**, 453-458.
- 60 (21) (a) T. C. Barros, S. Brochsztain, V. G. Toscano, P. B. Filho and M. J. Politi, *J. Photochem. Photobiol. A: Chem.* 1997, **111**, 97-104. (b) T. D. M. Bell, S. V. Bhosale, C. M. Forsyth, D. Hayne, K. P. Ghiggino, J. A. Hutchison, C. H. Jani, S. J. Langford, M. A. P. Lee and C. P. Woodward, *Chem. Commun.* 2010, **46**, 4881-4883. (c) D. Yan, A. Delori, G. O. Lloyd, T. Friščić, G. M. Day, W. Jones, J. Lu, M. Wei, D. G. Evans and X. Duan, *Angew. Chem. Int. Ed.* 2011, **50**, 12483-12486. (d) M. Pandeewar and T. Govindaraju, *RSC Adv.* 2013, **3**, 11459-11462.
- 65 (22) (a) I. Hisaki, T. Sasaki, K. Sakaguchi, W.-T. Liu, N. Tohna and M. Miyata, *Chem. Commun.*, 2012, **48**, 2219-2221. (b) I. Hisaki, T. Sasaki, N. Tohna and M. Miyata, *Chem. Eur. J.*, 2012, **18**, 10066-10073.
- 70

Graphical Abstract

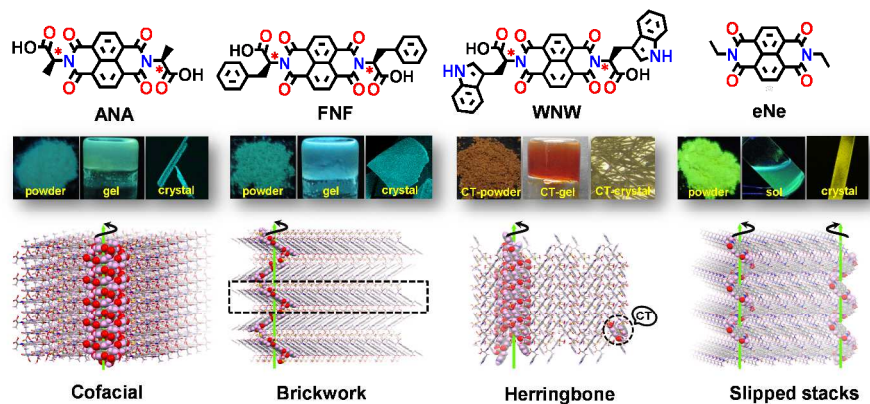
55

5 Biomimetic molecular organization of naphthalene diimide in the solid state: tunable (chiro-) optical, viscoelastic and nanoscale properties

60

M. Pandeeswar, Harshavardhan Khare, Suryanarayanarao
10 Ramakumar, and T. Govindaraju

65



15

70

20

25

30

35

40

45

50